

Bioinformatics Analysis of *ULK3* Gene in Prostate Cancer and Its Expression in DU145

Yuxuan Zou¹, Yunbo Zhang¹, Meng Sun¹, Mengjia Li^{1,2}, Yangyang Han^{1,2*}

¹Biology Teaching and Research Section, School of Basic Medical Sciences, Xinjiang Medical University, Urumqi 830017, China

²Xinjiang Key Laboratory of Molecular Biology for Endemic Diseases, Urumqi 830017, China

*Corresponding author: Yangyang Han, yyhan@xjmu.edu.cn

Copyright: © 2024 Author(s). This is an open-access article distributed under the terms of the Creative Commons Attribution License (CC BY 4.0), permitting distribution and reproduction in any medium, provided the original work is cited.

Abstract:

This study aimed to analyze the potential role of *ULK3* in prostate cancer (PCa) using bioinformatics methods and explore the effect of *ULK3* on the proliferation of prostate cancer cells by constructing a stable *ULK3*-knockdown prostate cancer cell line DU145. The expression of *ULK3* in PCa was analyzed using online databases TCGA and UALCAN. STRING database was utilized to analyze *ULK3*-related interacting proteins, and GSEA enrichment analysis was performed on differentially expressed genes of *ULK3*. The potential mechanism of *ULK3* was explored through GO and KEGG analyses. The microRNAs (miRNAs) regulating *ULK3* were predicted using the miRNet platform, and a potential *ULK3*-miRNA-mRNA regulatory network in PCa was constructed. The relationship between *ULK3* and immune infiltration in PCa was analyzed using the TIMER 2.0 database. Based on the above bioinformatics analysis, *ULK3* knockdown was performed in PCa cells DU145, and the downregulation efficiency of *ULK3* was detected by real-time quantitative PCR (RT-qPCR) and Western blot. The effects of stable downregulation of *ULK3* on the proliferation of prostate cancer cells were examined by scratch assay and MTT assay. The results showed that *ULK3* was highly expressed in PCa tissues compared to normal prostate tissues. Enrichment analysis revealed that *ULK3* expression was associated with various biological functions, with the main pathways being the Fanconi anemia pathway and the Notch signaling pathway. Immune infiltration analysis showed that the infiltration levels of multiple immune cells decreased significantly when *ULK3* was highly expressed. Furthermore, a prostate cancer cell line DU145 with *ULK3* knockdown was successfully constructed. Scratch assay and MTT assay demonstrated that *ULK3* knockdown inhibited the migration and proliferation of DU145 cells. These results suggest that *ULK3* plays an important biological role in prostate cancer, and its knockdown may have an inhibitory effect on PCa, providing new ideas for subsequent basic research and clinical treatment of PCa.

Keywords:

ULK3
Prostate cancer (PCa)
Bioinformatics
Lentivirus
Proliferation

1. Introduction

Prostate cancer (PCa) is the second most common type of malignant tumor among men globally. According to the latest cancer incidence statistics released in the United States in early 2024, the incidence of PCa among American men has been increasing year by year, with an annual rise of 3%^[1]. In China, the incidence of PCa has also been on the rise, accounting for about 25% of male cancer cases^[2]. Although surgical procedures, chemotherapy, and other treatment methods are currently available for PCa, and new drugs such as enzalutamide and abiraterone have demonstrated good efficacy in clinical settings, the development of resistance to these new drugs has become a significant clinical challenge, leading to poor prognosis for many patients^[3]. Tumor markers play a crucial role in the screening, diagnosis, and observation of treatment efficacy for PCa. Therefore, discovering the formation mechanism of PCa and its new molecular markers is essential for the treatment of PCa. Serine/threonine kinase Unc51-like kinase 3 (ULK3) is a member of the ULK family and plays a role in Shh (sonic hedgehog) signal transduction^[4]. Reports have found that abnormal expression of ULK3 is closely related to the occurrence and development of tumors such as bladder cancer and rhabdomyosarcoma: overexpression of ULK3 can promote the growth and metastasis of bladder cancer; overexpressed ULK3 has been detected in human rhabdomyosarcoma samples^[5,6]. Furthermore, a report on acute myeloid leukemia found that overexpression of ULK3 can promote autophagy and proliferation of leukemia cells and reverse the increased apoptosis induced by knocking down lncRNA HOTAIRM1^[7]. When studying the effects of ULK3 on squamous cell carcinoma, researchers analyzed the TCGA database and found that ULK3 is highly expressed in squamous cell carcinoma and its derived cell lines from different sites (including lung, cervix, etc.). The researchers also confirmed that when ULK3 is knocked down, the proliferation ability of squamous cell carcinoma cells is inhibited^[8]. These studies suggest that ULK3 plays a role in tumor proliferation and metastasis, but the role of ULK3 in the occurrence and proliferation of prostate cancer has not been fully elucidated and requires further investigation. In this study, bioinformatics analysis was used to analyze the correlation between poor clinical

outcomes of PCa and high levels of ULK3. Protein-protein interaction (PPI) network analysis was performed to identify potential ULK3-related pathways. Additionally, a ULK3-shRNA lentiviral vector was constructed to establish a DU145 cell line with knocked-down ULK3, and changes in prostate cancer cell proliferation were observed. This provides new insights into the treatment of PCa.

2. Results

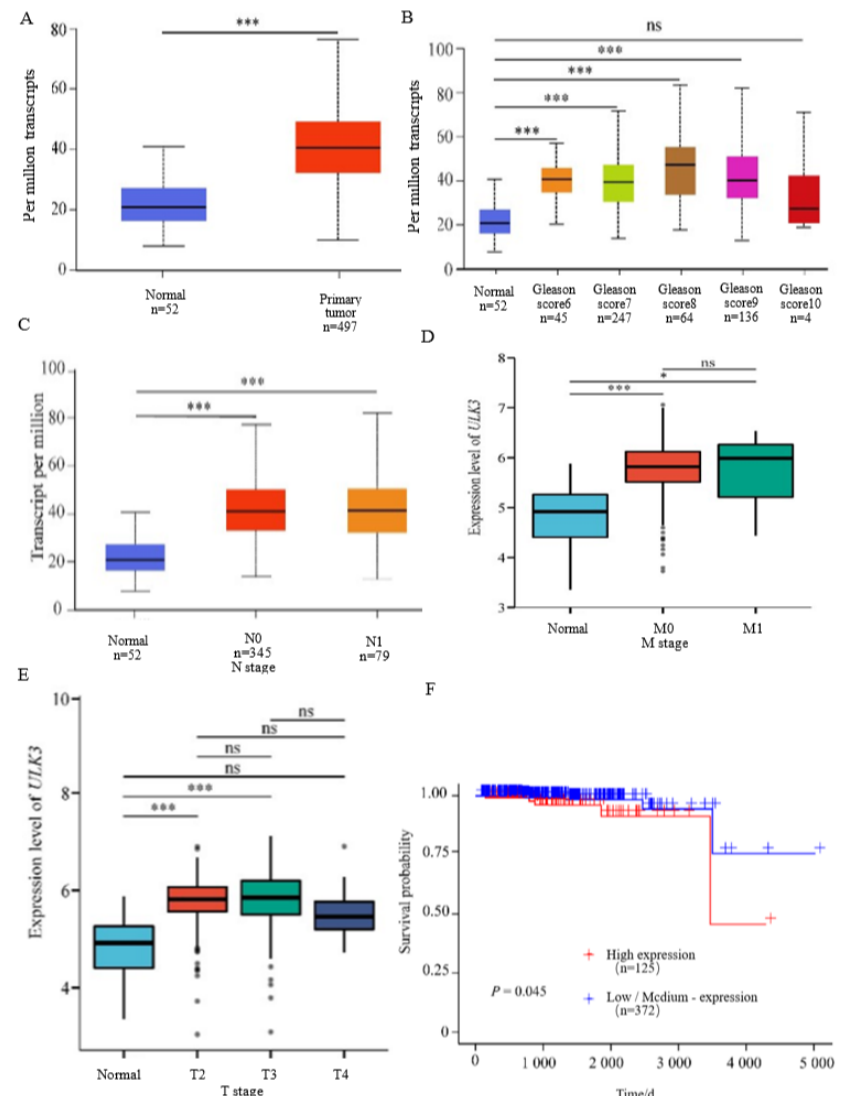
2.1. Relationship between ULK3 expression level and clinicopathological features of prostate cancer

Analysis using the UALCAN database revealed that the mRNA expression level of ULK3 in prostate cancer tissues was significantly higher than that in normal prostate tissues (**Figure 1A**). Among PCa tissues with different pathological features, the expression level of ULK3 was significantly elevated compared to normal prostate tissues (**Figure 1B**). The expression level of ULK3 in PCa, based on the TNM staging system (T stage, N stage, M stage), was significantly higher than that in the control group (**Figure 1C–1E**). Examination of the impact of different expression levels of ULK3 on the prognostic survival rate of PCa patients showed that patients with high ULK3 expression levels had a significantly lower survival rate ($P < 0.05$) (**Figure 1F**).

2.2. PPI network construction and GSEA enrichment analysis

The protein-protein interaction network (PPI) related to ULK3 was obtained from the STRING database (**Figure 2A**), where SUFU and STK36 were found to have close associations with ULK3. Clinical samples from the TCGA database were divided into high and low ULK3 expression groups, and a differentially expressed gene dataset was obtained from these two groups for gene set enrichment analysis (GSEA). The results are shown in the figure (**Figure 2B**): different colored lines represent the biological functions of ULK3 in PCa, reflecting its regulation of various signaling pathways. ULK3 was mainly involved in biological processes such as the transport of mature transcripts to the cytoplasm, tRNA processing, mRNA processing, capping intron processing

Figure 1. Expression level and clinical relevance of *ULK3*. (A) mRNA expression levels of *ULK3* in normal prostate tissue and prostate cancer; (B) mRNA expression levels of *ULK3* in prostate cancer patients with different gleason scores; (C) mRNA expression levels of *ULK3* in prostate cancer with different nodal metastasis status; (D) The expression level of *ULK3* in different M stages of prostate cancer; (E) The expression level of *ULK3* in different T stages of prostate cancer; (F) Analysis of the influence of the level of *ULK3* expression on the survival rate of prostate cancer patients, the red line represents the prognosis survival rate when *ULK3* is highly expressed, and the blue line represent the prognosis survival rate when *ULK3* is low/moderately expressed. * indicates $P < 0.05$; *** indicating $P < 0.001$; ns indicates $P > 0.05$.



containing mRNA precursors, and transcription termination of RNA polymerase II in the KEGG signaling pathway.

2.3. Enrichment analysis of the *ULK3* co-expression network

GO functional enrichment analysis and KEGG pathway enrichment analysis were performed using the Enrichr platform. The results of GO enrichment analysis indicated that *ULK3* and its co-expressed genes are mainly involved in biological processes such as dosage compensation via inactivation of the X chromosome, intraflagellar transport particle B assembly, negative regulation of gene silencing by RNA, positive regulation of histone H3-K27 methylation, and negative regulation of post-transcriptional gene silencing (Figure 3A). The

main cellular components involved include the STAGA complex, sex chromosome, TORC1 complex, AP-1 adaptor complex, and X chromosome (Figure 3B). The primary molecular functions involve chromatin insulator sequence binding, JUN kinase binding, DNA N-glycosylase activity, glycogen binding, and oxalate transmembrane transporter activity (Figure 3C). KEGG pathway enrichment analysis revealed that *ULK3* is mainly involved in Fanconi anemia and the Notch signaling pathway.

2.4. Construction of the potential *ULK3*-miRNA-mRNA regulatory network

miRNet was utilized to predict miRNAs targeting *ULK3* and multiple potential targets. ENCORI was then used to analyze the correlation between the expression of these

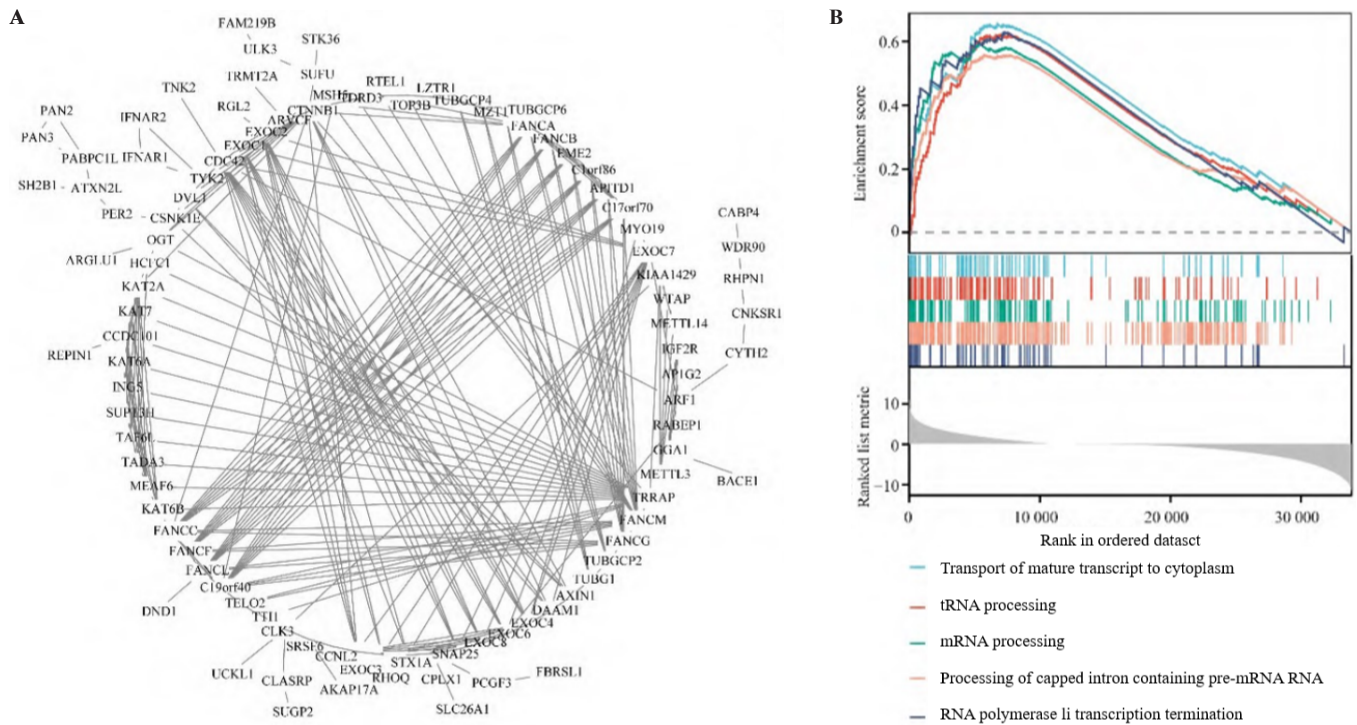


Figure 2. Protein interaction network and gene enrichment analysis of ULK3. (A) ULK3-related proteins and protein interaction networks; (B) Gene enrichment analysis of ULK3-related genes.

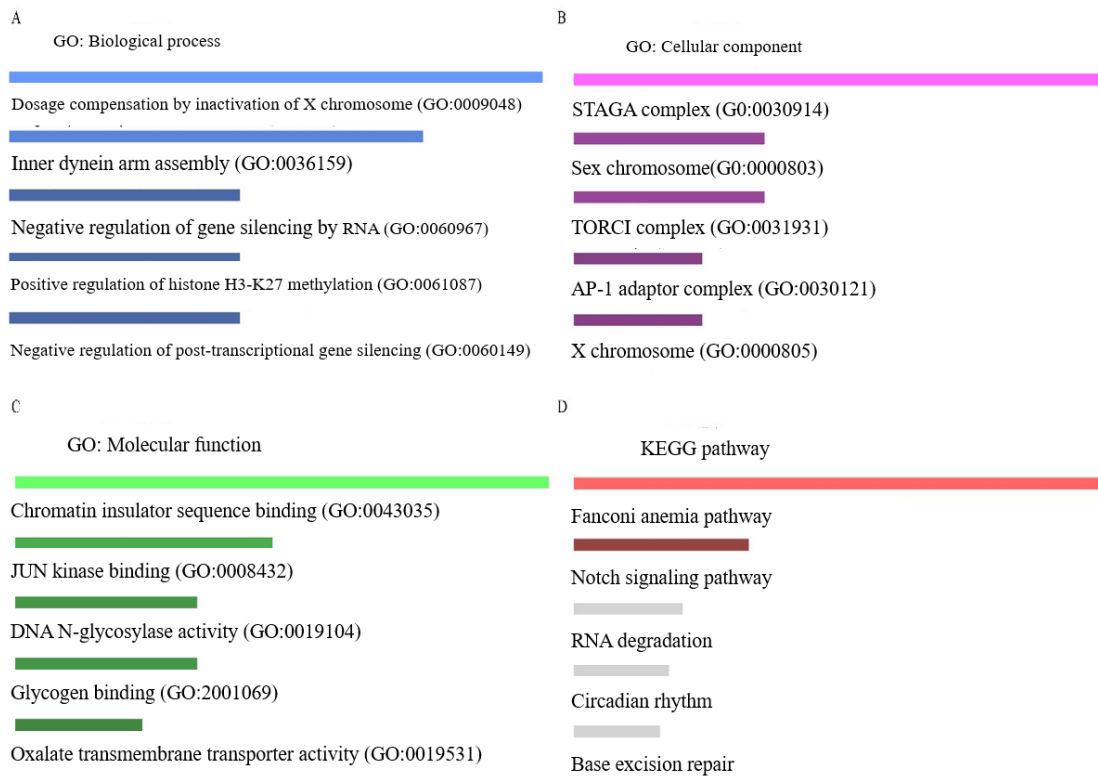


Figure 3. GO and KEGG enrichment analysis of ULK3 co-expressed genes. (A) GO enrichment analysis through biological processes; (B) GO enrichment analysis based on cell composition; (C) GO enrichment analysis through molecular functions; (D) Enrichment analysis of KEGG pathway for ULK3 co-expressed genes.

miRNAs and ULK3 mRNA in PCa. Among them, six miRNAs (miR-24-3p, miR-152-3p, miR-181c-5p, miR-196a-5p, miR-221-3p, and miR-222-3p) were negatively correlated with ULK3. Analysis of the expression levels of these six miRNAs in PCa revealed that their expression was significantly lower in PCa compared to normal prostate tissues (Figure 4A–4F).

2.5. Relationship between ULK3 and immune cell infiltration in PCa

The relationship between ULK3 expression in PCa and tumor immune infiltration was analyzed through the TIMER 2.0 database. As shown in the figure, after conducting immune infiltration analysis on the low ULK3 expression level group and the high ULK3 expression

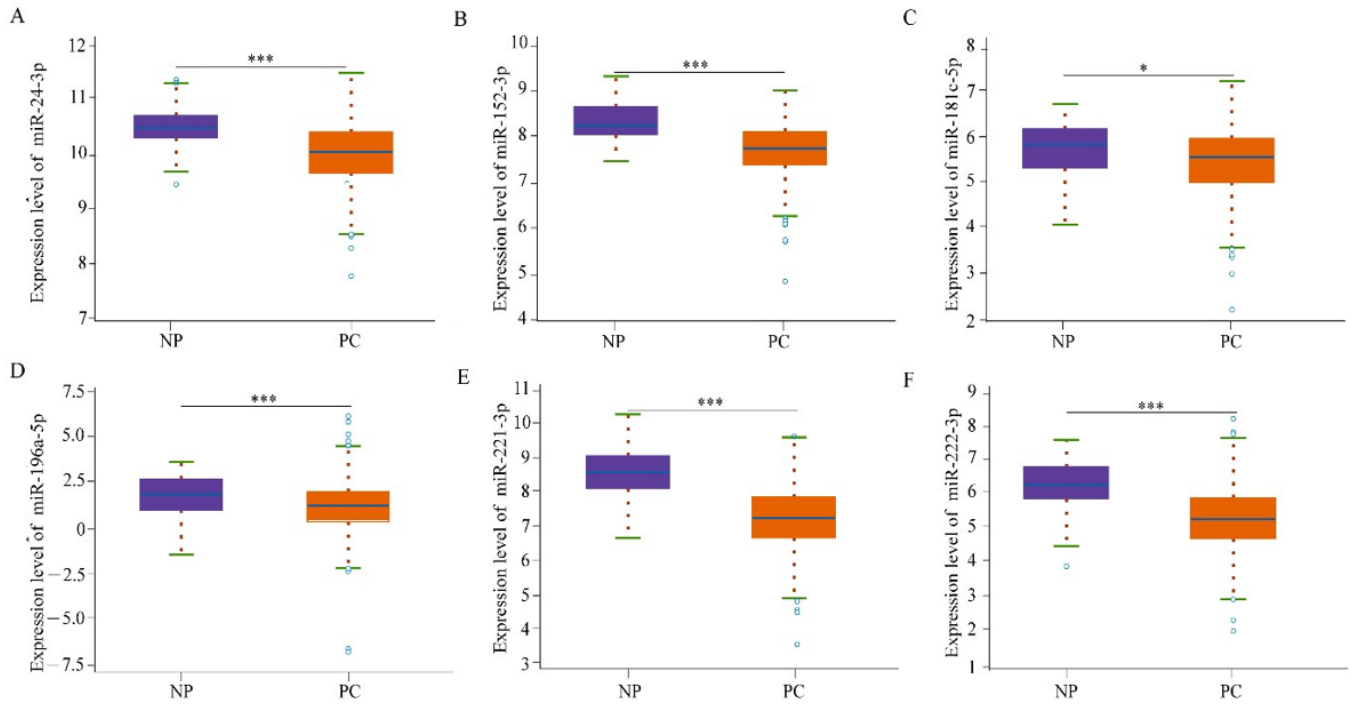


Figure 4. Construction of potential regulatory network for ULK3-miRNA-mRNA. (A) The expression levels of miR-24-3p in normal prostate tissue and prostate cancer; (B) The expression levels of miR-152-3p in normal prostate tissue and prostate cancer; (C) The expression levels of miR-181c-5p in normal prostate tissue and prostate cancer; (D) The expression levels of miR-196a-5p in normal prostate tissue and prostate cancer; (E) The expression levels of miR-221-3p in normal prostate tissue and prostate cancer; (F) The expression levels of miR-222-3p in normal prostate tissue and prostate cancer. * indicates $P < 0.05$; *** indicating $P < 0.001$. NP indicates normal prostate tissue; PC indicates prostate cancer tissue.

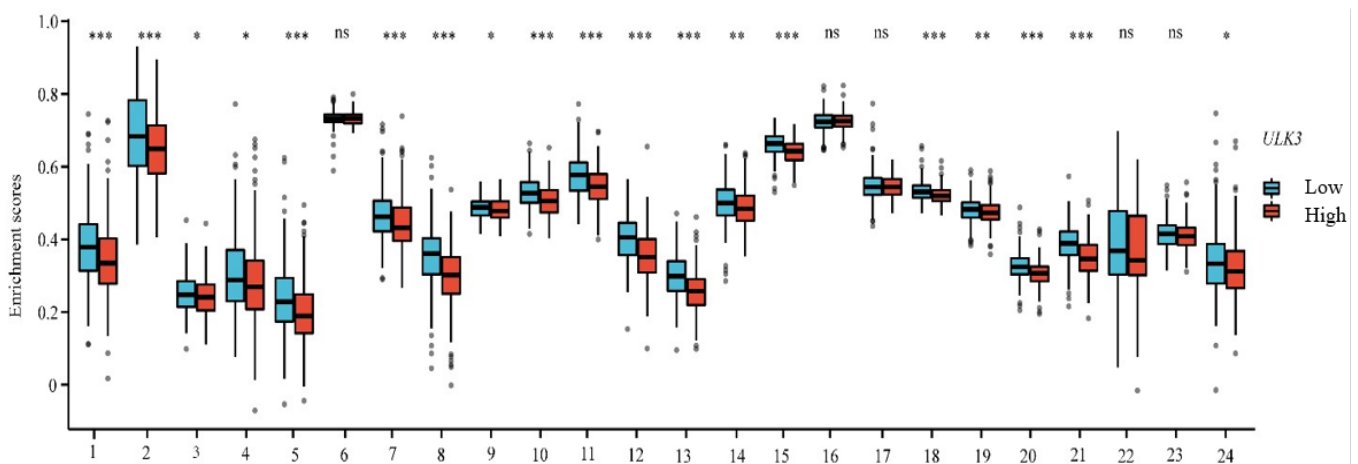


Figure 5. Correlation analysis between ULK3 and immune infiltration. (T cells; pDC; NK CD56dim cells; aDC; B cells; CD8 T cells; Cytotoxic cells; DC; Eosinophils; iDC; Macrophages; Mast cells; Neutrophils; NK CD56bright cells; NK cells; T helper cells; Tcm; Tem; TFH; Tgd; Th1 cells; Th17 cells; Th2 cells; Treg). * indicates $P < 0.05$; ** indicates $P < 0.01$; *** indicating $P < 0.001$; ns indicates $P > 0.05$.

level group, it was found that apart from CD8+T cells, T helper cells, central memory T cells (Tcm), T helper 17 cells (Th17 cells), and T helper 2 cells (Th2 cells), whose expressions showed no statistically significant difference between the groups, the expressions of other immune cells were significantly reduced in the high ULK3 expression group compared to the low ULK3 expression group ($P < 0.05$) (Figure 5).

2.6. Construction and verification of DU145-ULK3-shRNA stable cell lines

ULK3-shRNA lentiviral vectors were constructed by designing ULK3-shRNA-oligo primers, and sequencing comparison showed that the interference sequence was completely consistent with the design, indicating the successful construction of the lentiviral vector. The ULK3-shRNA lentiviral vector was packaged to obtain lentiviral supernatant, which was then used to infect DU145 cell lines. DU145-ULK3-shc and DU145-ULK3-shRNA (ULK3-sh1/sh2) stable cell lines were successfully selected using puromycin (Figure 6A).

Real-time quantitative PCR (RT-qPCR) was used to detect the mRNA levels of ULK3 in ULK3-shc, ULK3-shRNA1, and ULK3-shRNA2 (ULK3-sh1/sh2) cells. The results showed that compared with ULK3-shc, the expression of ULK3 in DU145 cells was significantly downregulated after infection with ULK3-shRNA ($P < 0.01$) (Figure 6B). Western blot analysis demonstrated

that the protein levels of ULK3 in the ULK3-shRNA1 and ULK3-shRNA2 groups were significantly downregulated compared to the ULK3-shc group ($P < 0.05$) (Figure 6C and Figure 6D). These results indicate that DU145 cell lines with knocked-down ULK3 have been successfully constructed.

2.7. Effects of knocking down ULK3 gene on the proliferation and migration activity of DU145 cells

Cell viability was measured in the control and experimental groups using the MTT assay. The results showed that the cell survival rates in the ULK3-shRNA1 and ULK3-shRNA2 (ULK3-sh1/sh2) groups were significantly lower than those in the ULK3-shc group. Specifically, the ULK3-sh1 group had an 11% decrease ($P < 0.01$) and the ULK3-sh2 group had a 15% decrease ($P < 0.05$) compared to the control group (Figure 7A). The scratch assay was used to assess cell wound healing ability, and the results indicated that the scratch wound healing rates in the experimental groups were significantly lower than those in the control group. Both the ULK3-sh1 and ULK3-sh2 groups showed a 21% decrease compared to the control group ($P < 0.05$) (Figure 7B and Figure 7C). These findings suggest that the expression of ULK3 may affect the proliferation and migration of DU145 cells.

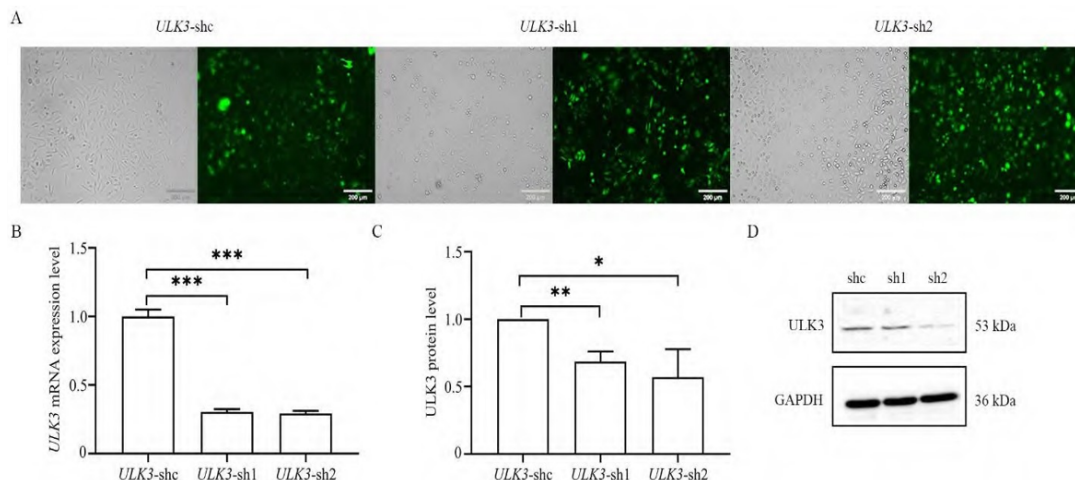


Figure 6. Construction and validation of DU145-ULK3-shRNA stable transfection cell line. (A) Fluorescence profile of DU145-ULK3-shRNA stable transgenic cell line; (B) Detect the mRNA expression levels of ULK3 in the control group ULK3-shc and experimental group ULK3-shRNA1 and ULK3-shRNA2 (ULK3-sh1/sh2); (C) Quantitative map of protein levels of ULK3 in control group ULK3-shc and experimental group ULK3-sh1/sh2; (D) Western blot analysis of ULK3 protein detection in control group ULK3-shc and experimental group ULK3-sh1/sh2. * indicates $P < 0.05$; ** indicates $P < 0.01$; *** indicates $P < 0.001$.

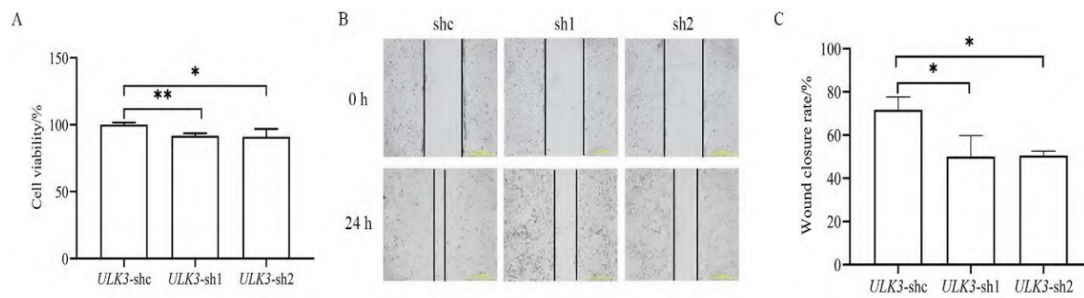


Figure 7. The effect of ULK3 knockdown on DU145 cells. (A) MTT assay to detect cell proliferation activity in control group ULK3-shc and experimental group ULK3-sh1/sh2; (B) Detection of migration distance of ULK3-shc in the control group and ULK3-sh1/sh2 in the experimental group at 0 h and 24 h through wound healing experiments; (C) Statistics on the wound closure of ULK3-shc cells in the control group and ULK3sh1/sh2 cells in the experimental group in the wound healing experiment. * indicates $P < 0.05$; ** indicates $P < 0.01$.

3. Discussion and conclusion

Serine/threonine kinase ULK3 plays a critical role in autophagy initiation, and the upregulation of ULK3 can enhance autophagy. It belongs to the ULK family along with ULK1 and ULK2 [9]. Previous studies have shown that ULK3 overexpression promotes cancer cell proliferation in bladder cancer and squamous cell carcinoma [6,9]. However, there is limited research on the specific functions of ULK3 in prostate cancer. Through online database analysis using TCGA and UALCAN, this study found that ULK3 expression is higher in prostate cancer tissues compared to adjacent normal tissues. This finding is similar to previous reports of high ULK3 expression in human muscle sarcomas and squamous cell carcinomas [5,9]. By analyzing the impact of ULK3 expression levels on the prognostic survival rate of PCa using the UALCAN database, it was discovered that patients with high ULK3 expression have a lower prognostic survival rate. This result aligns with reports on the prognosis of colorectal cancer patients [10] but contradicts the prognosis of patients with head and neck squamous cell carcinoma [11]. Through the construction of a protein-protein interaction network, it was identified that the fusion suppressor SuFu (suppressor of fused) and serine/threonine kinase 36 STK36 (serine/threonine kinase 36) have close associations with ULK3. The fusion suppressor SuFu can block the autophosphorylation of ULK3 and abolish its ability to phosphorylate and positively regulate GLI proteins [13]. STK36, also a member of the ULK family, is considered similar to the serine/threonine kinase fusion protein Fu in the Hedgehog signaling pathway [14].

Recent reports have found that STK36 overexpression significantly enhances the proliferation, invasion, and migration of PCa cells and reduces their sensitivity to docetaxel [15]. Gene enrichment analysis revealed that ULK3 expression is associated with biological processes such as the transport of mature transcripts to the cytoplasm, tRNA processing, and mRNA processing. Goruppi et al. (2023) found that ULK3 depletion through gene silencing or loss reduces the proliferation and clonogenic capacity of human keratinocytes and squamous cell carcinoma-derived cells, affecting transcription related to stem cells and metabolic programs [8]. Co-expression genes of ULK3 were obtained through UALCAN database analysis, and GO functional enrichment analysis and KEGG pathway enrichment analysis were performed. These co-expression genes were found to participate in various biological processes. The KEGG pathway enrichment analysis identified the Fanconi anemia pathway and Notch signaling pathway as the main pathways influenced by ULK3. While there have been no previous reports linking ULK3 to these two pathways, there is a wealth of research on ULK3's involvement in the sonic hedgehog (Shh) pathway. The Notch signaling pathway has been reported to play a crucial role in the development and progression of cancers such as lung cancer, gastric cancer, and hepatocellular carcinoma [16–18]. Abnormal activation of Shh signal transduction occurs in various cancers, including prostate cancer [19]. Existing research indicates that ULK3, as a self-phosphorylating kinase, can regulate GLI proteins, mediators of Shh signal transduction, and participate in the Shh pathway as a positive regulator of GLI

proteins. ULK3 can directly phosphorylate GLI proteins, enhancing their transcriptional activity and promoting the nuclear translocation of GLI1^[12]. Additionally, ULK3 can regulate GLI proteins through the activation of the Hedgehog pathway, promoting malignant behaviors such as proliferation and migration in bladder cancer^[6]. The Shh signaling pathway controls various developmental processes by regulating cell proliferation and differentiation and is associated with tissue homeostasis maintenance and stem cell proliferation^[20]. Simultaneously, the Shh signaling pathway is closely related to tumor proliferation. For instance, the Shh signaling pathway in liver cancer tumor-initiating cells can be activated by the Par-3 family cell polarity regulator (PARD3), driving liver cancer proliferation^[21]. The anticancer drug sulforaphane (SFN) negatively regulates the proliferation of leukemia stem-like cells by affecting the Shh signaling pathway^[22]. These findings suggest that ULK3 may participate in cancer initiation or progression through these biological processes and signaling pathways.

By constructing a ULK3-miRNA-mRNA interaction network, six potential miRNAs were identified that may regulate the expression of ULK3. The expression levels of these six miRNAs were found to be lower in PCa compared to normal prostate tissues, providing a new direction for further exploring the mechanism of ULK3 in PCa. These miRNAs have been reported to be associated with the regulation of tumor growth: miR-221-3p and miR-222-3p are related to the growth regulation of glioblastoma, where the atypical cadherin FAT1 can inhibit the tumor-promoting effect of PDCD10 through the RelA/miR221-3p/222-3p axis^[23]. Studies have also found that miR-196a-5p can promote the development of estrogen-dependent endometrial cancer by regulating FOXO1^[24]. Additionally, lncRNA FOXCUT affects the proliferation and migration of breast cancer by competitively binding to miR-24-3p and preventing the degradation of p38^[25]. miR-152-3p not only upregulates ULK3 expression through sponging with lncRNA HOTAIRM to promote autophagy and proliferation in leukemia cells, but it can also be regulated by circRNA Circ_0000284, affecting the expression of pyruvate dehydrogenase kinase 1 and promoting the growth and metastasis of intrahepatic cholangiocarcinoma^[7,26].

In this study, by analyzing the relationship between ULK3 and immune infiltration, it was found that the expression levels of multiple immune cells were significantly reduced when ULK3 was highly expressed. This suggests that ULK3 may be involved in the regulation of the PCa tumor microenvironment. Changes in immune cell expression levels play an important role in cancer development. For example, dendritic cells (DC cells) are abundant in gliomas with isocitrate dehydrogenase (IDH) type 1 mutations. However, IDH mutations in gliomas can lead to dendritic cell dysfunction through paracrine reprogramming of infiltrating monocytes. Dysfunctional dendritic cells limit the response of antigen-specific T cells in gliomas, thereby affecting the progression of the disease^[27]. Although natural killer (NK) cells can preferentially target cancer stem cells in several solid tumors other than prostate cancer, recent reports have found that NK cells can also preferentially target prostate cancer stem-like cells through the TRAIL/DR5 pathway^[28]. Furthermore, recent studies have shown that radiotherapy significantly increases the infiltration of various immune cells in prostate cancer patients undergoing neoadjuvant androgen deprivation therapy. The use of androgen deprivation therapy or radiotherapy as a single treatment significantly increases the number of T helper 1 (Th1) cells and regulatory T (Treg) cells, which is important for combining immunotherapy methods with current PCa therapies^[29].

Lentiviruses are highly effective tools in current cellular and model organism experiments^[30]. In this study, a lentiviral vector for ULK3 knockdown was constructed, and a stable ULK3-knockdown prostate cancer DU145 cell line was established through lentiviral infection. This facilitated further exploration of the role of ULK3 in PCa cell proliferation and migration. Rapid and uncontrolled proliferation of cancer cells in the body is one of their most important biological characteristics. Therefore, inhibiting cancer cell proliferation and growth and inducing cancer cell apoptosis play crucial roles in the treatment of various cancers^[31]. As mentioned earlier, high expression of ULK3 affects the development of cancers such as bladder cancer, leukemia, and squamous cell carcinoma, as well as cancer cell proliferation^[6-8]. In this study, knocking down ULK3 expression in PCa

cells significantly reduced the proliferation and migration abilities of DU145 cells. This is similar to the in vitro results reported by Liu et al. (2020) regarding the role of ULK3 in bladder cancer, where overexpression of ULK3 promoted the proliferation and metastasis of bladder cancer.

In summary, through a series of bioinformatics analyses, this study explored the expression level of ULK3 in prostate cancer, analyzed the biological processes that ULK3 may be involved in, and constructed a ULK3-miRNA-mRNA interaction network. This provides a certain direction for further research on the mechanism of ULK3 in PCa. By constructing a stable ULK3-knockdown DU145 cell line, the relationship between ULK3 expression levels and the proliferative capacity of DU145 cells was initially demonstrated. This lays a foundation for further revealing the relationship between ULK3 and the occurrence and development of prostate cancer and provides potential research directions.

4. Materials and methods

4.1. Materials and reagents

Cells and plasmids: The vector plasmid PLKO.1-EGFP-puro, as well as the helper plasmids pLP VSVG and galpol-midi, are all self-preserved plasmids in the laboratory. HEK 293T and DU145 cells were purchased from Wuhan Servicebio Technology Co., Ltd.

Reagents: Trans5 α (a strain of *Escherichia coli*), plasmid miniprep kit, gel extraction kit, FlyCut buffer, T4 DNA Ligase, restriction enzymes Age I and EcoR I (all from Beijing TransGen Biotech Co., Ltd.); 5 \times annealing buffer (Beijing Solarbio Science & Technology Co., Ltd.); DNA marker (Jiangsu Kangweishiji Biotech Co., Ltd.); RPMI-1640 basic medium, DMEM medium, 0.25% trypsin, penicillin-streptomycin, and protein loading buffer (all from Wuhan Servicebio Technology Co., Ltd.); TRIzol and transfection reagent Lipo3000 (both from Thermo Fisher Scientific, USA); 5 \times Lentivirus concentration solution (Beijing Pulilai Gene Technology Co., Ltd.); polybrene (Shanghai Beyotime Biotechnology Co., Ltd.); protein quantification kit (Sangon Biotech (Shanghai) Co., Ltd.); rabbit anti-human ULK3 polyclonal antibody and rabbit anti-GAPDH antibody (both from Hangzhou HuaAn Biotechnology Co.,

Ltd.); puromycin, protein pre-stained marker, and MTT (3-(4,5-Dimethylthiazol-2-yl)-2,5-Diphenyltetrazolium Bromide) reagent (all from Hefei Lanjieke Technology Co., Ltd.); Leica DMI8 fluorescence inverted microscope (from Leica Microsystems, Germany); quantitative PCR-specific reverse transcription reagents PrimeScript RT and TB Green Premix Ex Taq (Tli RNaseH Plus) (both from TAKARA, Japan); DMSO (Dimethyl sulfoxide) (from Sigma-Aldrich, Germany).

4.2. Bioinformatics analysis

Utilize the TCGA (<http://cancergenome.nih.gov/>) database to download PCa mRNA expression and clinical data; Use UALCAN (<https://ualcan.path.uab.edu/index.html>) to analyze the mRNA expression level of ULK3 in PCa and the impact of ULK3 expression on the survival rate of PCa patients; Compare the transcription levels of ULK3 in prostate cancer tissues and normal samples, as well as in different stages, using gene expression data from the TCGA database; Divide the clinical samples from the TCGA database into high and low ULK3 expression groups to obtain a differentially expressed gene dataset for the two groups, and visualize the results of GSEA enrichment analysis using the R package ggplot2 ($|NES| > 1$, $P < 0.05$, $Q < 0.05$, $P \text{ adj.} < 0.01$); Perform GO and KEGG enrichment analysis on co-expressed genes through the Enrichr platform (<http://amp.pharm.mssm.edu/Enrichr/>), with the graphing standard quantified by $-\log_{10} P$ and a threshold combined score of 0–300; Analyze protein-protein interactions using the STRING (<https://string-db.org>) database; Predict potential miRNAs that regulate ULK3 using the miRNet (<https://www.mirnet.ca/>) database, and validate the correlation between miRNA and ULK3 expression using the ENCORI database; Analyze the enrichment differences between ULK3 expression and various immune infiltrating cells through the Correlation module of the TIMER 2.0 database (<http://timer.cistrome.org/>).

4.3. Construction of lentiviral plasmid

The sequence of the target gene ULK3 (NM_001099436.4) was searched through NCBI. The interfering sequences for the target gene were designed using the website (<https://rnaidesigner.thermofisher.com/rnaexpress/>), with ULK3-shRNA1 sequence

being 5'-CGTGAAGTGGTAGCCATAAAGTGTG-3' and ULK3-shRNA2 sequence being 5'-TGGCGCGTGTCTTCATGCAGCAATT-3'. Based on these interfering sequences, ULK3-shRNA-oligo primers were designed and synthesized by Shanghai Sangon Biotech. The shRNA double strands were annealed using 5 × Annealing buffer. The PLKO.1-EGFP-puro plasmid was digested at AgeI and EcoRI sites, and the purified product was ligated with the annealed product. The ligation mixture was then transformed into Trans5α bacteria, spread on LB plates with ampicillin resistance, and incubated at 37°C for 12–16 hours. Colonies were picked, cultured, and sequenced. The PLKO.1-EGFP-puro-ULK3-shRNA plasmid was extracted using an endotoxin-free mini-prep kit and stored at -20°C.

4.4. Construction of stable ULK3 knockdown cell line

293T cells were seeded in a 10 cm cell culture dish one day before transfection, and transfection was performed when the cell density reached 70–80%. Before transfection, the culture medium of 293T was replaced with 6 mL of DMEM without antibiotics. The PLKO.1-EGFP-puro-ULK3-shRNA plasmid and helper plasmids (pLP VSVG and galpol-midi) were transfected into 293T cells using Lipo3000. Supernatants were collected at 48 and 72 hours post-transfection. The collected supernatants were filtered twice using a 0.45 μm filter membrane, and virus particles were concentrated according to the instructions of the 5 × virus precipitation concentration solution. After removing the supernatant, the lentivirus particles were resuspended and dissolved in 2 mL of PBS and stored at 4°C.

DU145 cells were seeded in a 12-well plate and infected with the corresponding concentrated virus and 8 μg/mL polybrene when the cell density reached 60%. The experiment was divided into control groups (ULK3-shc) and experimental groups (ULK3-shRNA1 and ULK3-shRNA2), with infection times set at 24, 48, and 72 hours. The infection efficiency was recorded using a fluorescence microscope at 24, 48, and 72 hours post-infection. After 72 hours, cells were selected with 1.2 μg/mL puromycin and expanded. Finally, cells were maintained in a medium containing 0.5 μg/mL puromycin.

4.5. RT-qPCR detection of ULK3 mRNA expression level in stable transfected cells

DU145 cells from the control group (ULK3-shc) and experimental groups (ULK3-shRNA1 and ULK3-shRNA2) were collected. Cells were lysed using TRIzol to extract RNA, which was then reverse-transcribed into cDNA. Real-time fluorescent quantitative PCR was used to detect the mRNA expression level of ULK3 in each group of cells, with GAPDH as the internal reference. Primer sequences were as follows: ULK3-F (5'-GAAGGACACTCGTGAAGTGGT-3'); ULK3-R (5'-ACAATGTGGGGATGTCGAATG-3'); GAPDH-F (5'-GGAAGGTGAAGGTCGGAGTCA-3'); GAPDH-R (5'-GTCATTGATGGCAACAATATCCACT-3'). Reaction conditions were 95°C for 30 seconds; 95°C for 15 seconds; 60°C for 34 seconds; and 40 cycles. The mRNA expression level of ULK3 was calculated using the 2-ΔΔCt method.

4.6. Western blot detection of ULK3 protein level in stable transfected cells

Cells from the three groups were collected and lysed with RIPA lysis buffer for 30 minutes on ice, shaking the culture dish every 5 minutes. The lysed cells were then collected into EP tubes. After centrifugation, protein quantification was performed using the Bradford method, and samples were mixed with 5 × loading protein buffer and boiled. The protein level of ULK3 was detected using 8% SDS-PAGE gel electrophoresis, followed by membrane transfer and blocking. Primary antibodies against ULK3 and GAPDH were used for incubation at 4°C overnight. After washing three times with PBST, secondary antibodies were incubated for 1 hour, followed by three washes with PBST and color development. Grayscale value analysis was performed using Image J.

4.7. Scratch assay to detect cell migration ability

Cells in the logarithmic growth phase were seeded in dishes. When cell density reached 70–80%, a 200 μL pipette tip was used to scratch lines in the dish. Microscope images were taken to record cells at 0 and 24 hours. Image J was used to measure cell migration distance, and the wound healing rate was calculated for the control and experimental groups.

4.8. MTT assay to detect cell viability

Cells in logarithmic growth phase were seeded in a 96-well plate with 4000 cells per well. After 44 hours of culture, MTT reagent was added. After incubating at 37°C for 4 hours, DMSO was added 30 minutes before the end of the incubation to terminate the reaction. Absorbance at 490 nm was measured using a microplate reader.

4.9. Statistical analysis

Statistical analysis was performed using Graphpad Prism 8.0 software. Measurement data conforming to a normal distribution were expressed as mean \pm standard deviation (SD). The *t*-test was used for comparison between groups, and $P < 0.05$ indicated a statistically significant difference.

Funding

National Natural Science Foundation of China (Project No.: 82260493); Full-time Innovative Talents Fund of the Tianchi Program for High-level Talents in Xinjiang Uygur Autonomous Region

Disclosure statement

The authors declare no conflict of interest.

References

- [1] Siegel R, Giaquinto AN, Jemal A, 2024, Cancer Statistics, 2024. CA: A Cancer Journal for Clinicians, 74: 12–49.
- [2] Xia CF, Dong XS, Li H, et al., 2022, Cancer Statistics in China and United States: Profiles, Trends, and Determinants. Journal of Chinese Medicine, 135(5): 584–590.
- [3] Sekhoacha M, Riet K, Motloung P, et al., 2022, Prostate Cancer Review: Genetics, Diagnosis, Treatment Options, and Alternative Approaches. Molecules, 27(17): 5730.
- [4] Kasak L, Näks M, Eek P, et al., 2018, Characterization of Protein Kinase ULK3 Regulation by Phosphorylation and Inhibition by Small Molecule SU6668. Biochemistry, 57(37): 5456–5465.
- [5] Kawabata N, Ijiri K, Ishidou Y, et al., 2011, Pharmacological Inhibition of the Hedgehog Pathway Prevents Human Rhabdomyosarcoma Cell Growth. International Journal of Oncology, 39(4): 899–906.
- [6] Liu BB, Gao WY, Sun W, et al., 2020, Promoting Roles of Long Non-Coding RNA FAM83H-AS1 in Bladder Cancer Growth, Metastasis, and Angiogenesis Through the c-Myc-Mediated ULK3 Upregulation. Cell Cycle, 19(24): 3546–3562.
- [7] Jing YP, Jiang XK, Lei L, et al., 2021, Mutant NPM1-Regulated lncRNA HOTAIRM1 Promotes Leukemia Cell Autophagy and Proliferation by Targeting EGR1 and ULK3. Journal of Experimental & Clinical Cancer Research, 40(1): 312.
- [8] Goruppi S, Clocchiatti A, Bottoni G, et al., 2023, The ULK3 Kinase is a Determinant of Keratinocyte Self-Renewal and Tumorigenesis Targeting the Arginine Methylome. National Communication, 14(1): 887.
- [9] Goruppi S, Procopio MG, Jo S, et al., 2017, The ULK3 Kinase is Critical for Convergent Control of Cancer-Associated Fibroblast Activation by CSL and GLI. Cell Reports, 20(10): 2468–2479.
- [10] Liu LY, Zhang JL, Liu HD, et al., 2021, Correlation of Autophagy-Related Genes for Predicting Clinical Prognosis in Colorectal Cancer. Biomarkers in Medicine, 15(10): 715–729.
- [11] Patel D, Dabhi A M, Dmello C, et al., 2022, FKBP1A Upregulation Correlates With Poor Prognosis and Increased Metastatic Potential of HNSCC. Cell Biology International, 46(3): 443–453.
- [12] Maloverjan A, Piirsoo M, Michelson P, et al., 2010, Identification of a Novel Serine/Threonine Kinase ULK3 as a Positive Regulator of Hedgehog Pathway. Experimental Cell Research, 316(4): 627–637.
- [13] Maloverjan A, Piirsoo M, Kasak L, et al., 2010, Dual Function of UNC-51-Like Kinase 3 (ULK3) in the Sonic Hedgehog

- Signaling Pathway. *Journal of Biological Chemistry*, 285(39): 30079–30090.
- [14] Maloverjan A, Piirsoo M, 2012, Mammalian Homologues of Drosophila Fused Kinase. *Vitamin and Hormone*, 88: 91–113.
- [15] He T, Li NX, Pan ZJ, et al., 2024, Serine/Threonine Kinase 36 Induced Epithelial-Mesenchymal Transition Promotes Docetaxel Resistance in Prostate Cancer. *Scientific Reports*, 14(1): 729.
- [16] Zheng H, Zhu XY, Gong EH, et al., 2023, Luteolin Suppresses Lung Cancer Progression Through Targeting the circ_0000190/miR-130a-3p/Notch-1 Signaling Pathway. *Journal of Chemotherapy*, 35(4): 330–342.
- [17] He Y, He PZ, Lu SM, et al., 2023, KIF3C Regulates the Progression and Metastasis of Gastric Cancer via Notch1 Pathway. *Digestive and Liver Disease*, 55(9): 1270–1279.
- [18] Zhou DZ, Cao SJ, Xie H, 2023, Research on Predicting the Occurrence of Hepatocellular Carcinoma Based on Notch Signal-Related Genes Using Machine Learning Algorithms. *Turkish Journal of Gastroenterology*, 34(7): 760–770.
- [19] Jeng KS, Chang CF, Lin SS, 2020, Sonic Hedgehog Signaling in Organogenesis, Tumors, and Tumor Microenvironments. *International Journal of Molecular Science*, 21(3): 758.
- [20] Zheng GD, Ren JX, Shang L, et al., 2023, Sonic Hedgehog Signaling Pathway: A Role in Pain Processing. *Neurochemical Research*, 48(6): 1611–1630.
- [21] Wu JY, Tan HY, Chan YT, et al., 2024, PARD3 Drives Tumorigenesis Through Activating Sonic Hedgehog Signalling in Tumour-Initiating Cells in Liver Cancer. *Journal of Experimental & Clinical Cancer Research*, 43(1): 42.
- [22] Wang FP, Huang XY, Sun YW, et al., 2022, Sulforaphane Regulates the Proliferation of Leukemia Stem-Like Cells via Sonic Hedgehog Signaling Pathway. *European Journal of Pharmacology*, 919: 174824.
- [23] Malik N, Kundu A, Gupta Y, et al., 2023, Protumorigenic Role of the Atypical Cadherin FAT1 by the Suppression of PDCD10 via RelA/miR221-3p/222-3p Axis in Glioblastoma. *Molecular Carcinogenesis*, 62(12): 1817–1831.
- [24] Zhu YZ, Tang YF, Fan YH, et al., 2023, MiR-196a-5p Facilitates Progression of Estrogen-Dependent Endometrial Cancer by Regulating FOXO1. *Histology & Histopathology*, 38(10): 1157–1168.
- [25] Yu XF, Qian FZ, Zhang XQ, et al., 2024, Promotion Effect of FOXCUT as a MicroRNA Sponge for miR-24-3p on Progression in Triple-Negative Breast Cancer Through the p38 MAPK Signaling Pathway. *Chinese Medical Journal*, 137(1): 105–114.
- [26] Sun J, Feng ML, Zou HL, et al., 2023, Circ_0000284 Facilitates the Growth, Metastasis, and Glycolysis of Intrahepatic Cholangiocarcinoma Through miR-152-3p-Mediated PDK1 Expression. *Histology & Histopathology*, 38(10): 1129–1143.
- [27] Friedrich M, Hahn M, Michel J, et al., 2023, Dysfunctional Dendritic Cells Limit Antigen-Specific T Cell Response in Glioma. *Neuro-Oncology*, 25(2): 263–276.
- [28] Seki T, Shimizu Y, Ishii K, et al., 2021, NK Cells Can Preferentially Target Prostate Cancer Stem-Like Cells via the TRAIL/DR5 Signaling Pathway. *Biomolecules*, 2021, 11(11): 1702.
- [29] Erlandsson A, Lundholm M, Watz J, et al., 2023, Infiltrating Immune Cells in Prostate Cancer Tissue After Androgen Deprivation and Radiotherapy. *International Journal of Immunopathology and Pharmacology*, 37: 3946320231158025.
- [30] Liu QZ, Wei LD, Liu L, et al., 2023, The Analysis of Pan-Cancer FDFT1 Gene Expression With Cancer Prognosis, and Its Impact on the Proliferation of Various Tumor Cells. *Journal of Youjiang Medical University for Nationalities*, 45(4): 563–569.
- [31] Liu XR, He Y, Chen Y, et al., 2023, Construction of Chronic Myeloid Leukemia K562 Cell Line With Overexpression of Human TCRP1 Gene Based on Lentivirus Vector and Its Biological Function Detection. *The Journal of Practical Medicine*, 39(19): 2456–2460.

Publisher's note

Whioce Publishing remains neutral with regard to jurisdictional claims in published maps and institutional affiliations.